

Electromagnetic Field Simulation for ICRF Antenna and Comparison with Experimental Results in LHD

Takashi MUTOH, Hiroshi KASAHARA, Tetsuo SEKI, Kenji SAITO,
Ryuhei KUMAZAWA, Fujio SHIMPO and Goro NOMURA

National Institute for Fusion Science, 322-6 Oroshi-cho, Toki 509-5292, Japan

(Received 8 January 2010 / Accepted 26 February 2010)

Ion cyclotron range of frequencies (ICRF) heating antennas in LHD are numerically simulated and analyzed by HFSSTM finite-element electromagnetic wave field calculation code. The model includes an accurate vacuum chamber wall of LHD and ICRF antenna structure and a simple model of plasma in a helical configuration. Antenna coupling with plasma is simulated by an artificial freshwater volume with enhanced high permittivity of $\epsilon = 500\text{--}2000$. RF current distribution and electromagnetic field distribution on and near the ICRF antenna are analyzed and well elucidated through a comparison with the experimental results. The frequency dependence of experimental loading resistance can be simulated by the calculation, and the RF dissipation on the antenna structure is studied and compared with experimental results. The local high heat load around gaps between the carbon side protectors is well explained, and the effect of gap distance is studied. Comparison with the experimental results reveals that the ICRF heating in the LHD, including the antenna and helical plasma, is well simulated by commercial HFSSTM code analysis. It will also be useful for future improvements in ICRF antenna design in helical devices.

© 2010 The Japan Society of Plasma Science and Nuclear Fusion Research

Keywords: ICRF antenna, RF heating, LHD, helical device, HFSS code, electromagnetic wave

DOI: 10.1585/pfr.5.S2104

1. Introduction

Ion cyclotron range of frequencies (ICRF) heating method is considered as one of the most promising technologies for heating future fusion devices. The optimization of antennas for physics and technological applications is very important to build up an efficient, high-power heating system. Normally the R&D process requires many experiences of plasma heating experiments, and a long time is needed to optimize antenna design. In helical systems, high power ICRF heating experiment is now testing only one device in LHD [1–4]. Therefore, numerical simulation is very helpful to optimize antenna design, because the experimental trial of any change to the antenna structure is very limited. To improve the plasma coupling and stand-off voltage, numerical code calculation is beneficial and is needed to save time in the R&D process. In this paper, numerically calculated results of antenna coupling, heat load due to dissipated RF power, and electromagnetic field distribution are studied and compared with experimental observations. The electromagnetic field calculation code, called HFSS (High-Frequency Structure Simulator, HFSSTM [5]), is used for this purpose. The code is a commercial finite element method calculation code and is widely used to analyze microwave and high-frequency circuits.

The ICRF antennas in an LHD vacuum chamber

shown in Fig. 1 are located on the outer side of the toroid [6]. The chamber has a complicated helical structure, as



Fig. 1 Two sets of ICRF antennas are set on the outer side of toroid in the LHD vacuum chamber. They are positioned in front of the superconducting helical windings.

author's e-mail: mutoh@nifs.ac.jp

the figure shows. The positions of the cyclotron resonances and fast-wave cutoff surfaces of the LHD are quite unique and different [1, 2] from those of tokamaks. The poloidal cross section of plasma has an oval shape and rotates along the helical structure to the toroidal direction. The antenna front surface is three-dimensionally twisted to fit the scrape-off layer of the helical LHD plasma. One pair of loop antennas is composed of two separate antennas each of which has a single current strap and is independently fed from the top and bottom vacuum ports, respectively. The Faraday shield pipes are inclined to cancel the electric field along the confinement magnetic field lines, as shown in Fig. 1.

2. Simulation Model and Antenna Coupling Characteristics

Electromagnetic field calculation using 3-D HFSS simulation code was carried out on a finely detailed model of the LHD ICRF antennas and surrounding hardware. The realistic configuration included precise replications of the twisted antenna conductors, inclined Faraday screen, and carbon side protectors. The LHD vacuum chamber wall of stainless steel was also realistically modeled and included. Figure 2 shows the calculation model of the ICRF antenna and LHD vacuum chamber. The chamber of a 1/10 torus section is included, and both ends of the toroidal cut are defined as the free radiation boundaries for the electromagnetic wave. The LHD plasma model is composed of a freshwater material with artificial permittivity instead of real plasma. Fresh water is a better material as dielectric absorbing material for simulation model than salt water which used in many calculations. Using the salt water, the electromagnetic field emitted from antenna is shielded by high electric conductivity and it cannot propagate inside of plasma area. As described later, fresh water with high permittivity behaves as a good plasma model to simulate the natural antenna-coupling characteristics.

The RF electromagnetic field and current distribution are calculated on and near the ICRF antenna and are shown in Fig. 3. The left figure shows the current intensity contour on the front surface of the current strap, and the right figure shows the propagated wave magnetic field intensity distribution on the horizontal plane. Simulation results show that the RF current flows mainly near the edge of the antenna current strap, while a small portion flows on the central area of the strap. The standing wave is excited in the model of fresh water volume, as shown in the right figure. These wave field patterns resemble the plasma wave analysis results of TASK-WM code, with similar standing wave numbers and wavelengths [7]. This model uses fresh-water material with artificial high permittivity, which has a homogeneous and isotropic dielectric characteristic. A more realistic absorber model should include anisotropic and inhomogeneous dielectric properties due to the magnetic field direction and plasma parameter dependences. Those absorber characteristics should be included in future improved models.

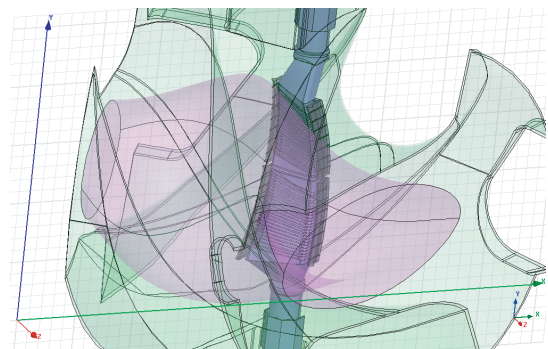


Fig. 2 Calculation model of the ICRF antennas and LHD vacuum chamber for the HFSS electromagnetic wave field simulation. A tenth of LHD section is included and the plasma model is composed of fresh water with artificially high permittivity.

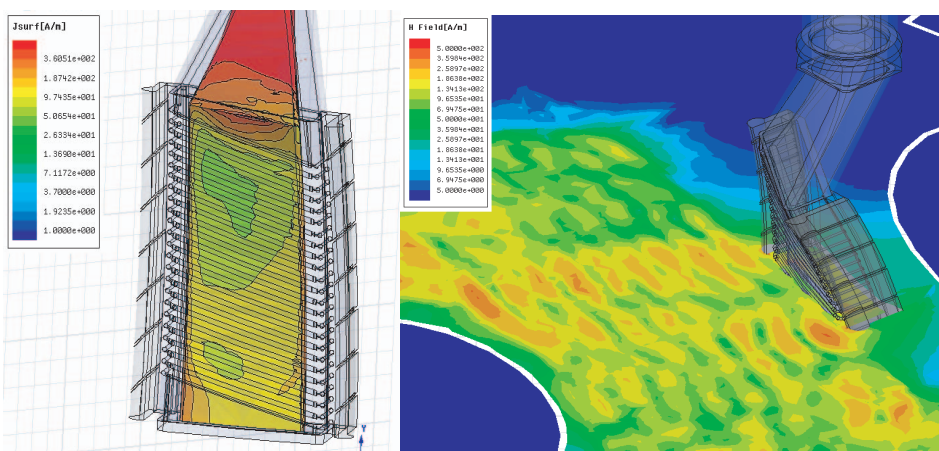


Fig. 3 RF current distribution on the front surface of current strap (left) and excited wave peak intensity on the horizontal plane in the plasma model (HFSS code calculation with 39 MHz and $\epsilon = 2000$).

The coupling characteristics of the ICRF antenna and plasma can be estimated by the loading resistance derived from the voltage standing wave ratio (VSWR) along the transmission line in HFSS code calculation. Antenna loading resistance is significantly varied by changing the operating frequency in the heating experiment, as shown in Fig. 4. The frequency was changed from 25 to 44 MHz to apply the various heating modes in the LHD experiment. The loading resistance was increased by changing the frequency as shown, and the data for six antennas are plotted in the figure. The plasma density and temperature profiles and the distance between the antennas and the plasma are also effective parameters, but the frequency dependence was the most effective factor in the heating experiment. At a frequency of approximately 25 MHz, it was difficult to launch high power to the plasma due to the low antenna loading resistance. The calculation results of the HFSS code are also shown in the figure by red closed circles. These calculated values are smaller than the experimental values. The difference should be attributed to the incomplete model of the plasma in which fresh water was used as

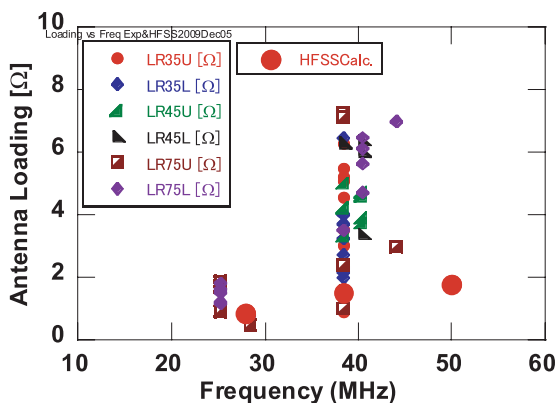


Fig. 4 Antenna loading resistances in various frequency experiments in LHD are shown. Experimental data of six antennas and calculated data by HFSS code are shown.

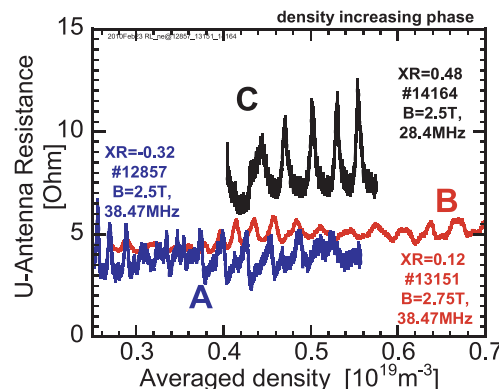
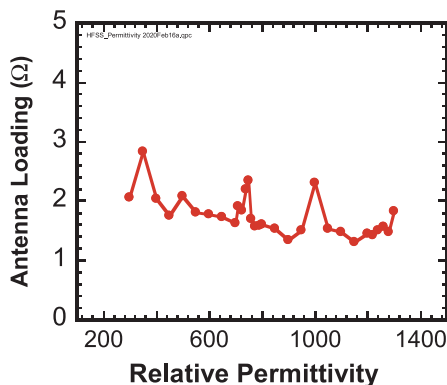


Fig. 5 Eigenmode couplings of antenna are appeared in the HFSS simulation calculation (left) and also in the LHD plasma experiment (right). In the experiment, ion cyclotron resonance positions are different in three different resonant position cases of A, B and C [8].

the model material. Although the absolute values are a little small, a relative increasing tendency is well reproduced by the simulation calculation.

As shown in Fig. 3, excited waves have a standing wave form inside a plasma area. The standing wave form is defined by the reflective boundary conditions, wavelength, and dissipation rate inside the wave travelling medium. In the plasma experiment, the wave travelling area is inside the right-hand cutoff surface of fast wave. The wavelength is decided mainly by the plasma density, and the dissipation rate is decided by the damping mechanism, which depends on the cyclotron damping and Landau damping conditions. By changing the plasma density gradually, the antenna coupling changes periodically when the mode number of standing waves is changed. This property is recognized as the Eigenmode structure, as shown in Fig. 5 (right) [8]. The Eigenmode appears strongly if the damping rate is small (case C), which means the Q value of cavity resonance is high.

This Eigenmode structure is also simulated by HFSS calculation by changing the permittivity value of artificial freshwater material for the plasma model. The permittivity is changed from 300 to 1300 for the calculation, as shown in Fig. 5 (left). Three discontinuous peaks are seen at the permittivity dependence, and they seemed to form an Eigenmode formation. The appearance of the Eigenmode in the wavelength dependence in the calculation shows that the coupling model between the antennas and plasma is quite realistic and reliable enough to proceed to further calculations.

3. RF Power Dissipation Analysis for Long Pulse Operation

The estimation of RF power dissipation on the antenna structure is the most beneficial application of the simulation. On the long-pulse plasma operation sustained by ICRF power, temperature increased at the operated antennas. Figure 6 shows visible and IR camera screens during a

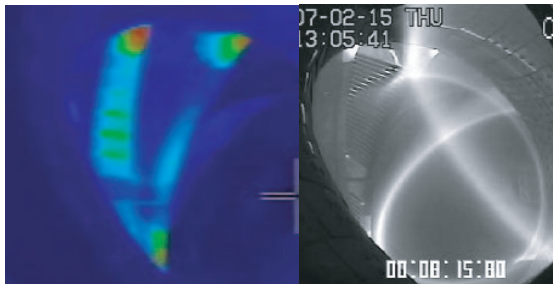


Fig. 6 Screen pictures of IR (left) and visible (right) cameras for the ICRF antenna inside of the LHD vacuum chamber during the steady state operation of 8 minutes.

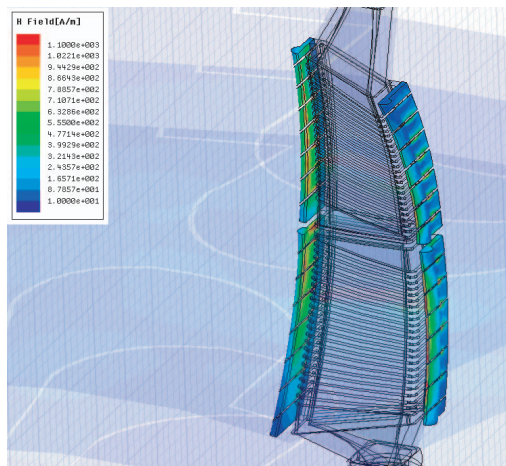


Fig. 7 RF Magnetic field intensity (H) on the carbon protectors of ICRF antenna is shown by color contour plot. Power dissipation on the carbon protector depends on the H field intensity. Gap distances of carbon protectors are 8 mm in the upper antenna and 4 mm in the lower antenna. Real antenna gaps are set to 4 mm.

long-pulse operation exceeding 8 minutes. Although many hot spots are observed, the heat sources of these spots are not clear from this screen. From the calculation of HFSS code, the local increases in temperature of protectors can be explained by RF power dissipation at the inner edges and around the gaps between carbon plates. Figure 7 shows the calculated results of RF heat dissipation on the antenna structures. The major part of the heat dissipation is deposited at the carbon protectors, as the figure shows. Especially, an area of high heat deposition exists in the gaps between the carbon protectors. On the other hand, the hot spots of both edges of the uppermost carbon protectors cannot be explained by the RF dissipation calculation. These two hot spots should be attributed to the large heat flux from the plasma.

To see the effect of the gap distance, the gap distance of the upper antenna model is set to 8 mm and that of the lower antenna is set to 4 mm. The gap in the real antenna is 4 mm. The heat deposition is greater at the large distance antenna of 8 mm (upper antenna) than at that of

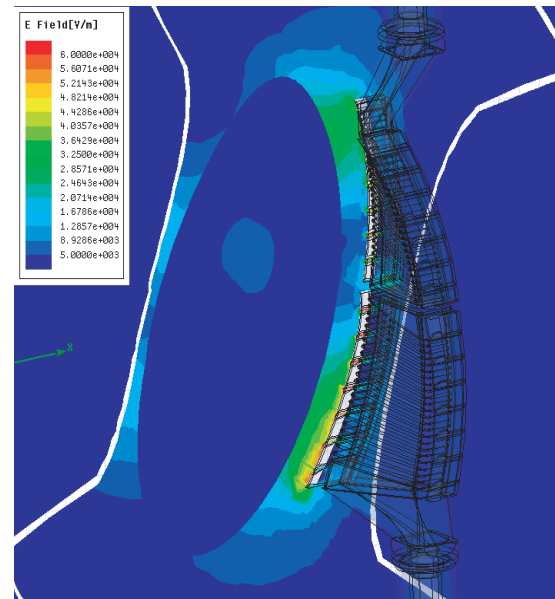


Fig. 8 RF electric field peak intensity (E) distribution is shown. E field is high at lower antenna having narrow gaps of 4 mm.

4 mm (lower antenna), as the figure shows. The calculated high heat deposition positions coincide well with the experimental observation in Fig. 6 (left). RF field dissipation heats the edge blades near the plasma and the gaps between the protectors. To reduce the local heating at the gaps, a small distance gap is better in the calculation. However, arcing prevention between the protector plates is another optimization factor.

Sometimes local RF arcing was observed in the gaps between carbon protector plates. The effect of the large gap distance is worse with the aspect of the power dissipation, as shown in Fig. 7, but the RF electric field intensity is reduced due to the large gap distance. The RF electric field intensity is calculated and compared between the upper and lower antennas. The electric field intensity of the 8 mm antenna is around half that of the 4 mm antenna. The electromagnetic wave field pattern outside the antenna structure is almost the same between these antennas despite the difference in gap. Therefore, the coupling properties projected to the loading resistance value are the same for either gap. The evaluation function to optimize the gap distance, and thus to increase the heating RF power in the steady state, is not simple.

4. Summary

The electromagnetic wave field near the ICRF antenna in LHD is numerically analyzed by HFSS finite element method calculation code. The model includes accurate LHD plasma shape, vacuum chamber wall, and ICRF antenna structures in a helical configuration. Plasma load is properly simulated using a model of artificial freshwater volume with enhanced high permittivity of $\epsilon = 300$ -2000.

RF current distribution and electromagnetic wave field distribution near the ICRF antenna are analyzed and well understood. The experimentally observed frequency dependence of loading resistance is explained by the calculation. And the plasma-coupling property, including Eigenmode excitation, can be simulated using the freshwater model. RF dissipation on the antenna structure is estimated and compared with the experimental results. The effect of the gap distance between carbon protectors is simulated, and the local heat load at the gaps is well explained and discussed to prevent arcing at the gaps. From the comparison of the calculation results with the experimental results, the HFSS code calculation is found to be useful for future improvements in antenna design even in complicated structures in helical devices.

Acknowledgements

The authors appreciate the experimental staff of LHD for their support and great efforts in the experiment. This

work is performed mainly under the budget codes of NIFS09ULRR504 and NIFS09ULRR525.

- [1] T. Mutoh, R. Kumazawa, T. Seki, K. Saito, H. Kasahara *et al.*, Nucl. Fusion **47**, 1250 (2007).
- [2] T. Mutoh, R. Kumazawa, T. Seki, T. Watari and K. Saito, Phys. Rev. Lett. **20**, 4533 (2000).
- [3] R. Kumazawa *et al.*, 22nd IAEA Fusion Energy Conf. EX/P6-29 (2008).
- [4] H. Kasahara *et al.*, 22nd IAEA Fusion Energy Conf. EX/P6-30 (2008).
- [5] Ansoft Announce HFSS v11, IEEE MTT-S INTERNATIONAL MICROWAVE SYMPOSIUM, HONOLULU, HI - June 5, 2007 http://www.ansoft.com/news/press_release/070605.cfm
- [6] T. Mutoh, R. Kumazawa, T. Seki *et al.*, J. Plasma Fusion Res. SERIES **1**, 334 (1998).
- [7] T. Yamamoto, S. Murakami and A. Fukuyama, Plasma Fusion Res. **3**, S1075 (2008).
- [8] T. Mutoh, R. Kumazawa, T. Seki, T. Watari, F. Shimpo and G. Nomura, J. Plasma Fusion Res. **77**, 495 (2001).